

Molecular Basis for Differential Patterns of Drug Resistance in Influenza N1 and N2 Neuraminidase

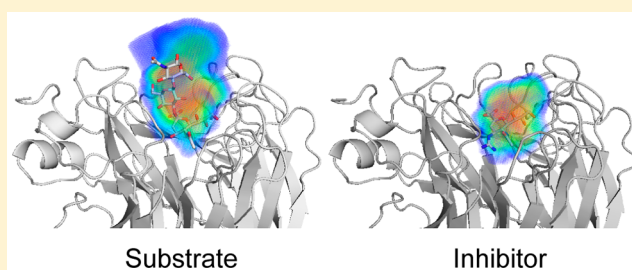
Kristina L. Prachanronarong,[†] Ayşegül Özen,^{†,∇} Kelly M. Thayer,^{‡,○} L. Safak Yilmaz,^{†,§} Konstantin B. Zeldovich,[‡] Daniel N. Bolon,[†] Timothy F. Kowalik,^{||} Jeffrey D. Jensen,[#] Robert W. Finberg,[⊥] Jennifer P. Wang,[⊥] Nese Kurt-Yilmaz,[†] and Celia A. Schiffer^{*,†}

[†]Department of Biochemistry and Molecular Pharmacology, [‡]Program in Bioinformatics and Integrative Biology, [§]Program in Systems Biology, ^{||}Department of Microbiology and Physiological Systems, and [⊥]Department of Medicine, University of Massachusetts Medical School, Worcester, Massachusetts 01605, United States

[#]School of Life Sciences, École Polytechnique Fédérale de Lausanne, 1015 Lausanne, Switzerland

Supporting Information

ABSTRACT: Neuraminidase (NA) inhibitors are used for the prevention and treatment of influenza A virus infections. Two subtypes of NA, N1 and N2, predominate in viruses that infect humans, but differential patterns of drug resistance have emerged in each subtype despite highly homologous active sites. To understand the molecular basis for the selection of these drug resistance mutations, structural and dynamic analyses on complexes of N1 and N2 NA with substrates and inhibitors were performed. Comparison of dynamic substrate and inhibitor envelopes and interactions at the active site revealed how differential patterns of drug resistance have emerged for specific drug resistance mutations, at residues I222, S246, and H274 in N1 and E119 in N2. Our results show that the differences in intermolecular interactions, especially van der Waals contacts, of the inhibitors versus substrates at the NA active site effectively explain the selection of resistance mutations in the two subtypes. Avoiding such contacts that render inhibitors vulnerable to resistance by better mimicking the dynamics and intermolecular interactions of substrates can lead to the development of novel inhibitors that avoid drug resistance in both subtypes.



INTRODUCTION

Seasonal influenza infects over 24 million people annually in the United States, contributing to 200,000 hospitalizations and 40,000 deaths.¹ Vaccines are partially effective in preventing influenza infection but can fail due to antigenic drift, a high viral mutation rate, and mismatches between vaccine and circulating strains of virus.^{2,3}

Direct acting antiviral agents, including neuraminidase (NA) inhibitors, are used to combat influenza infections.⁴ Influenza NA, a viral sialidase necessary for viral maturation, cleaves terminal sialic acid residues from glycoproteins to release the budding virus from the surface of infected cells.^{5–7} NA may also increase viral motility in mucus.⁸ In 1999, the U.S. Food and Drug Administration approved two competitive active site NA inhibitors, oral oseltamivir and inhaled zanamivir, and in 2014, a third agent, peramivir, was approved for intravenous administration.^{4,9–11}

Influenza NA is a homotetrameric transmembrane protein (Figure 1A), and sites of drug resistance are located both inside and outside of the active site (Figure 1B). Type A influenza is most prevalent and is divided into subtypes based on two surface proteins, hemagglutinin (HA) and NA, of which two subtypes predominate in human infection, N1 and N2.

Between N1 and N2, the residues in the active site are 94% identical, and overall, N1 and N2 share approximately 45% amino acid sequence identity and 60% similarity (see Methods). Influenza NA cleaves two types of human substrates, 3'-sialyl-*N*-acetylglucosamine and 6'-sialyl-*N*-acetylglucosamine (Figure 2A).^{12,13} The first substrate has α -2,3 glycosidic linkages between the terminal sialic acid and the neighboring galactose, and these substrates are present in avian gastrointestinal epithelium, human respiratory tract mucin, and human lower airway epithelium.¹³ The second substrate has α -2,6 glycosidic linkages, and these substrates are present in human upper airway epithelium.¹³ Oseltamivir, zanamivir, and peramivir have similar structures that mimic that of the substrate cleavage product, sialic acid (Figure 2B).

With the use of NA inhibitors in clinic, resistant viral variants have emerged in human patient isolates (Table 1).^{14–26} Structural and computational studies on resistant NA variants to date have focused on understanding how mutations cause weaker inhibitor binding, especially for oseltamivir resistance in the H1N1-2009 swine flu pandemic.^{27–29} Alterations of the

Received: July 14, 2016

Published: November 7, 2016

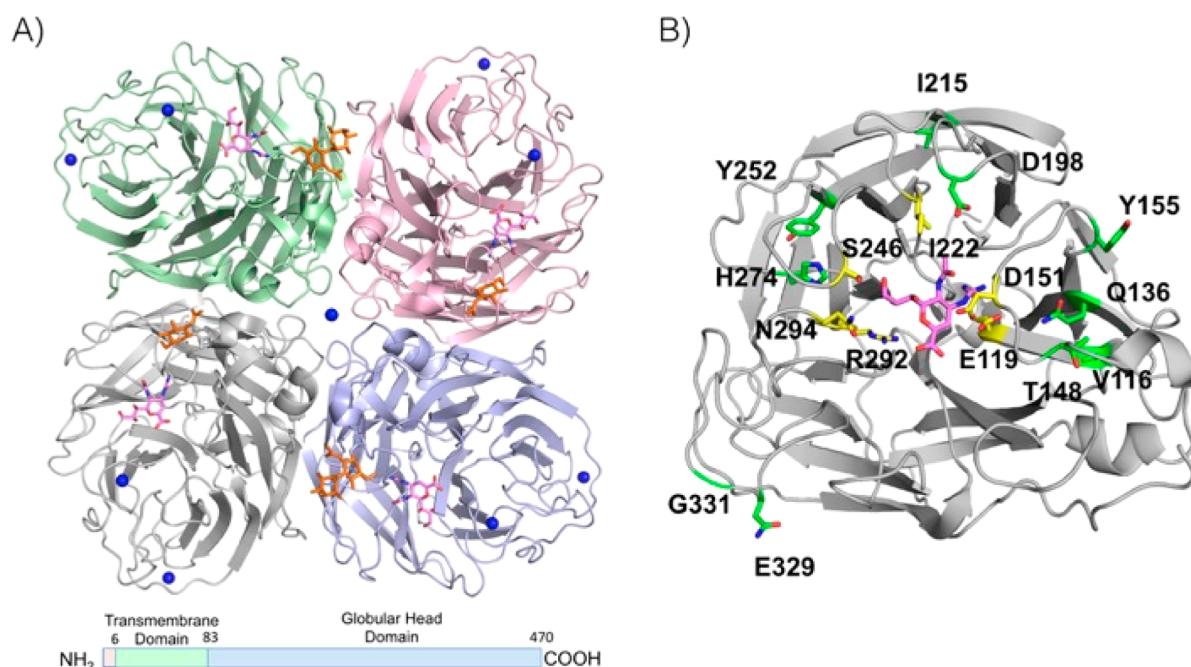


Figure 1. Influenza NA structure and sites of drug resistance. (A) The homotetrameric structure of NA globular head domains, where each monomer is in a distinct color, calcium ions in dark blue, glycosylation in orange, and the inhibitor zanamivir bound at the active site of each monomer is depicted as magenta sticks. (B) Residues that mutate to confer drug resistance are labeled on the NA structure (Table 1). Sites at the active site and making direct contacts with the inhibitor (magenta sticks) are in yellow, while those away from the active site are in green.

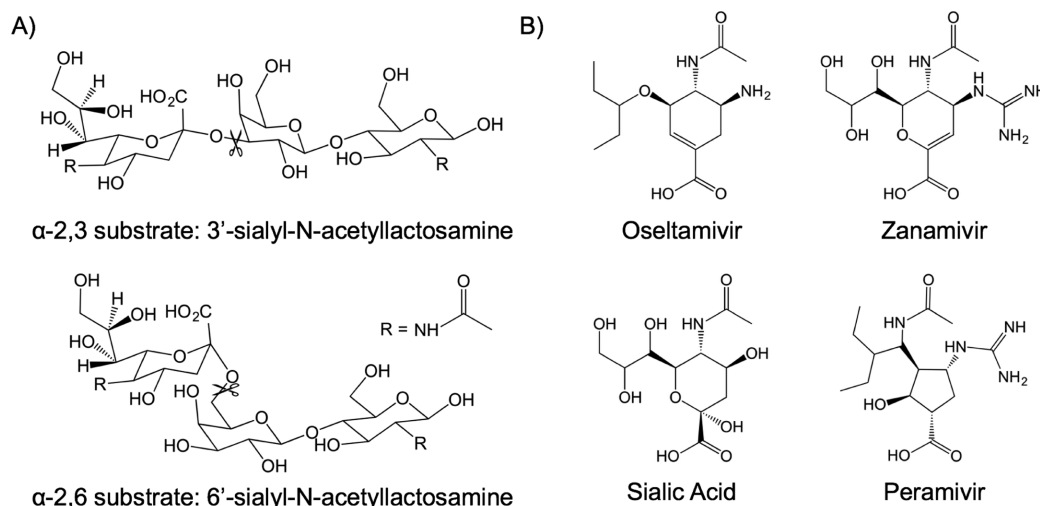


Figure 2. Chemical structure of NA substrates and inhibitors. (A) α -2,3 substrate, 3'-sialyl-N-acetylactosamine, and α -2,6 substrate, 6'-sialyl-N-acetylactosamine. Scissors indicate the location of the scissile bond. The R denotes an N-acetyl group. (B) Chemical structures of NA inhibitors and the substrate cleavage product sialic acid.

interactions of the active site E276 with the inhibitor have been proposed to be central mechanisms of drug resistance. Specifically, the clinically most prevalent H274Y mutation disrupts the strong interaction between the histidine and E276, causing a shift of the E276 side chain.²⁸ Thus, resistance appears to be acquired by subtle changes within the active site.

Despite highly homologous sialic acid binding active sites the patterns of resistance mutations that are observed in clinic for N1 versus N2 NA are not the same (Table 1). The H274Y mutation confers resistance to oseltamivir only in the N1 genetic background (754-fold increase),¹⁸ while E119V is observed only in N2 subtype isolates.^{30,31} The E119V NA mutation can also confer resistance to inhibitors in the N1

subtype, but this mutation is not selected as it significantly impairs viral fitness in N1.^{18,32} Unlike in N2, this impairment of viral fitness in N1 is most likely due to the mutation impacting substrate recognition. The differential selection of resistance mutations between subtypes has been largely overlooked for influenza NA and is fundamentally linked to the balance between substrate versus inhibitor binding.

Comparing the binding of substrates versus inhibitors in other viral drug targets has been very effective in revealing why particular mutations are selected and the underlying mechanism of drug resistance: Drug resistance in enzyme targets often occurs due to a change in molecular recognition such that drug resistant variants no longer bind inhibitors while still

Table 1. Drug Resistance Mutations in NA Subtypes N1 and N2^{a,b}

subtype N1	subtype N2
N70S ^Z	
V116A ^{OZ}	
Q 136R ^{ZP} /K ^{ZP}	E119 V^O/I^{OZP}
	Q 136 K ^Z
	T 148 K ^Z
D151E^{ZP}	
Y155H ^{OZP}	
D 198E ^O	
I222 V^O/L^O/R^{OZP}/T^O/K^O	
	V215I ^O
S246N^{OZ}/G^O	
H252Y ^O	
H274Y ^{OP}	
	R292 K^{OZP}
N294S^{OZP}	N294S ^O
	N329 K ^{OZ}
	S331R ^O

^aO,Z,P represent inhibitors oseltamivir, zanamivir, and peramivir, respectively; indicated if susceptible to a given mutation. ^bResidues in bold have direct contacts with the ligands analyzed in this study.

recognizing and processing substrates to carry out their biological function. Through our analysis of HIV-1 and Hepatitis C Virus (HCV) NS3/4A protease cocrystal structures, we established the substrate envelope hypothesis, explaining how substrates adopt a conserved shape when bound to the active site, which we termed the substrate envelope.^{33,34} Primary drug resistance mutations occur where inhibitors protrude beyond this substrate envelope and make contact with active site residues more extensively than the substrates.^{34,35} Mutations at such sites selectively negatively impact inhibitor binding over substrates, skewing the balance between inhibition versus substrate processing in favor of the substrate, hence causing drug resistance.

Alterations in protein dynamics between N1 and N2 may also contribute to differential patterns of drug resistance. The conformation and flexibility of the 150s loop at the active site has been proposed to differentiate N1 and N2 NA inhibitor binding and possibly selection of resistance mutations.³⁶ Previously, we incorporated conformational dynamics into a *dynamic* substrate envelope model using molecular dynamics (MD) simulations and compared inhibitors to substrates to effectively explain the drug resistance mechanism of active site mutations.^{37,38} These fundamental principles we learned from HIV-1 and HCV protease are generalizable to any drug target that evolves to confer resistance.³⁹ In the present study we apply this strategy to investigate why different resistance mutations are selected in influenza NA subtype 1 versus subtype 2.

Specifically, we investigate the molecular basis for the selection of differential patterns of drug resistance in N1 versus N2 NA, through a comparative structural and molecular dynamic analysis of substrates versus inhibitors in the two subtypes. MD simulations were performed on the full homotetrameric influenza NA subtypes N1 and N2 bound to two human substrates and the inhibitors oseltamivir and zanamivir to calculate dynamic inhibitor and substrate envelopes. In agreement with the substrate envelope hypothesis, the contacts of a specific inhibitor beyond those of

substrates in a given subtype underlie the susceptibility to drug resistance mutations at that position. Our results explain the molecular basis for subtype-specific resistance mutations and provide insights to guide the development of novel inhibitors to avoid drug resistance by better mimicking the dynamic binding features and molecular interactions of substrates with the NA active site.

RESULTS

NA strains from N1 and N2 subtypes with available high-resolution crystal structures and high (>90%) sequence identity to the subtype consensus sequence were selected (see [Methods](#) for details of strain selection criteria). Eight 100 ns explicitly solvated MD simulations were performed on the N1 and N2 tetrameric NA in complex with substrates and inhibitors ([Figure 2](#), [Table S1](#)). All MD simulations were performed on the full tetramer to simulate the biological unit with the added benefit of sampling ligand-protease dynamics in each monomeric unit. For each simulation, the root mean squared deviation (RMSD) calculations converge and remain stable ([Figure S1](#)). In addition, experimental and simulation derived B-factors and α carbon root mean squared fluctuation (RMSF) values agree well ([Figure S2](#)).

Dynamic Substrate and Inhibitor Envelopes. Dynamic substrate envelopes were defined by mapping the van der Waals (vdW) volumes of substrates in the active site over the simulation time on a three-dimensional grid ([Figure 3](#)). This calculation produces a probability distribution of conformers in the active site, providing more detail compared to static substrate envelopes. Similarly, the dynamic inhibitor envelopes for oseltamivir and zanamivir were calculated individually as bound to N1 and N2 NA ([Figure 3](#)). Overall, the inhibitors are smaller and more rigid than the substrates. Especially the solvent exposed carbohydrate moieties of the substrates have broader envelopes, as also reflected by the high root-mean-squared-fluctuation (RMSF) for these atoms ([Figure S3](#)). Thus, the dynamic envelopes capture the increased flexibility of substrates over inhibitors.

Alterations in Intermolecular Contacts Correlate with Differential Patterns of Drug Resistance in N1 and N2. To quantify the interaction of substrates and inhibitors with individual active site residues, vdW contact energies over the course of MD simulations were calculated ([Figure 4](#)). Mapping the variation between inhibitor versus substrate contacts onto the NA active site ([Figure 4A](#)) reveals that certain residues are contacted more by inhibitors than substrates and vice versa. The changes in intermolecular contacts of inhibitors versus substrates were then compared at the major drug resistance sites in the two NA subtypes.

Residue E119 is a site of primary drug resistance in N2 NA but not in subtype N1 ([Table 1](#)). This differential pattern is effectively explained by alterations in vdW interactions and hydrogen bonds in N1 versus N2 NA ([Figures 5A and 6](#)). E119 interacts with both substrate and inhibitor to a similar extent in N1 ([Figure 5A](#)), and, therefore, a mutation to decrease inhibitor's contacts at this residue would also impact substrate processing. Resistance mutations at this residue in N1 has not been observed clinically or through influenza surveillance,¹⁶ although mutations at 119 have been observed experimentally *in vitro* through reverse genetics and other *in vitro* mutagenesis studies.⁴⁰ E119 interacts with the C4-guanidinium group of zanamivir and peramivir and with the corresponding amino group on oseltamivir. Since E119 makes extensive contacts with

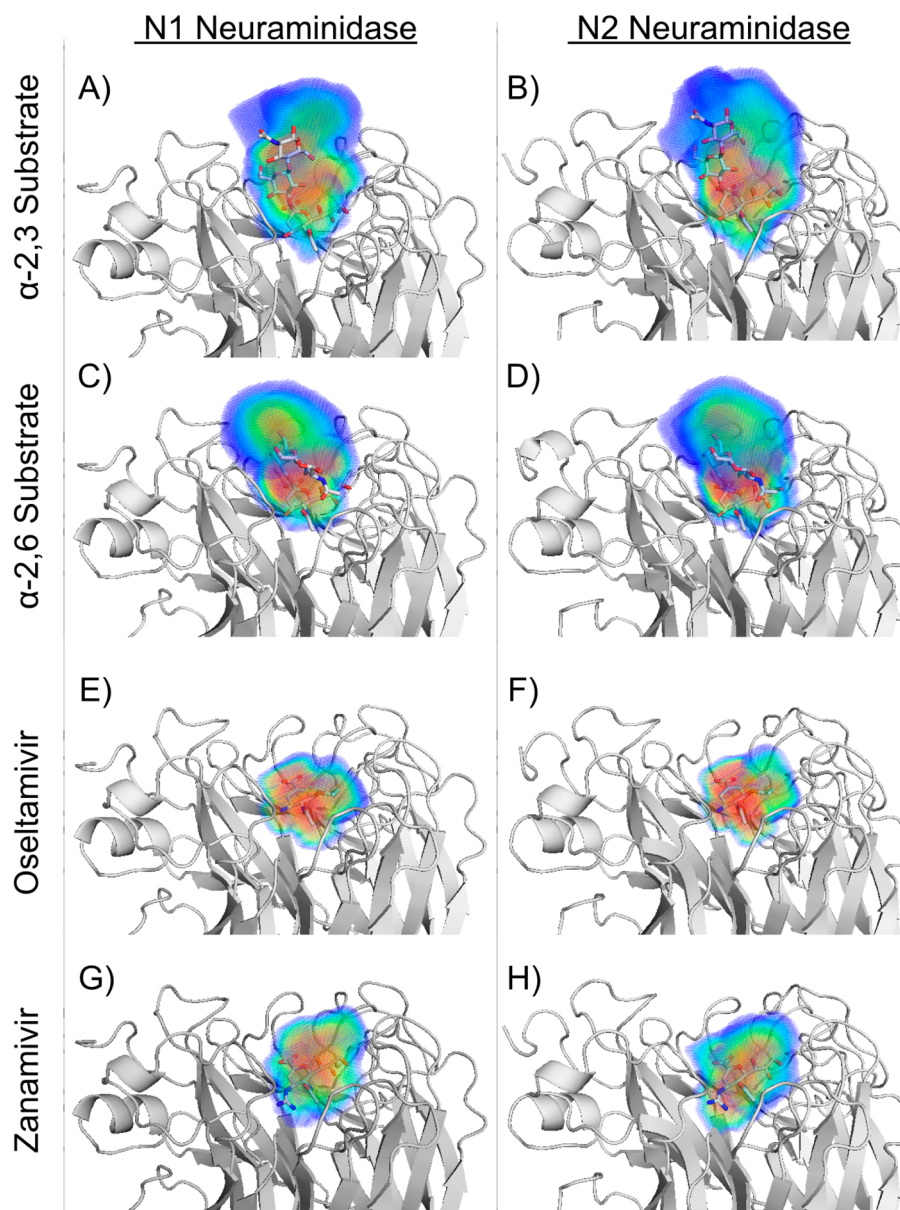


Figure 3. Dynamic substrate and inhibitor envelopes for N1 and N2 NA. The ligands are in gray sticks, and the probabilistic volume distribution for the envelopes is represented using a rainbow color spectrum from red to blue to indicate more to less occupied regions. The left and right columns are for subtypes N1 and N2 NA, respectively. Dynamic substrate envelope of (A, B) α -2,3 and (C, D) α -2,6 substrates and the inhibitor envelopes of (E, F) oseltamivir and (G, H) zanamivir.

substrates in N1, mutations at this site would confer strong fitness penalties that cannot be overcome even in the presence of inhibitor. Previous *in vitro* experimental results indeed support that E119 is critical for substrate binding and fitness in N1, and, therefore, E119 is not a prevalent drug resistance site in N1.⁴⁰

In contrast, in N2, both oseltamivir and zanamivir have more favorable vdW contacts than substrates, especially the α -2,6 substrate, indicating that a drug resistance mutation would be well tolerated at this location in N2 NA. Hydrogen bonds with inhibitors are also more prevalent at E119 compared to substrates (Figure 6) in N2, explaining why E119 is prone to mutation without compromising substrate recognition in N2 NA.

Residue I222 is a primary drug resistance site in N1 NA and is a secondary permissive mutation in N2 NA (Table 1).¹⁴ The

alterations in vdW contacts explain the prevalence of I222 mutations in the N1 subtype (Figure 5B): I222 contacts the *N*-acetyl group and the glycerol/pentyl-ether hydrophobic moieties in ligands. I222 has favorable vdW contacts with both substrate and inhibitors in N2, and therefore I222 is not an optimal site for mutation in N2. However, in N1, contacts of I222 are more favorable with the oseltamivir and zanamivir inhibitors compared to substrates. A resistance mutation would be well tolerated at this site and could weaken inhibitor binding much more than substrates. Since I222 does not appear to be critical for substrate binding in N1, mutations at this site confer strong fitness advantages in the presence of inhibitor.⁴⁰ In fact, I222 is considered to be a “hotspot” location for drug resistance mutations in N1, where many drug resistance mutations are well tolerated and provide wild type like fitness for N1 in the presence of oseltamivir.⁴⁰

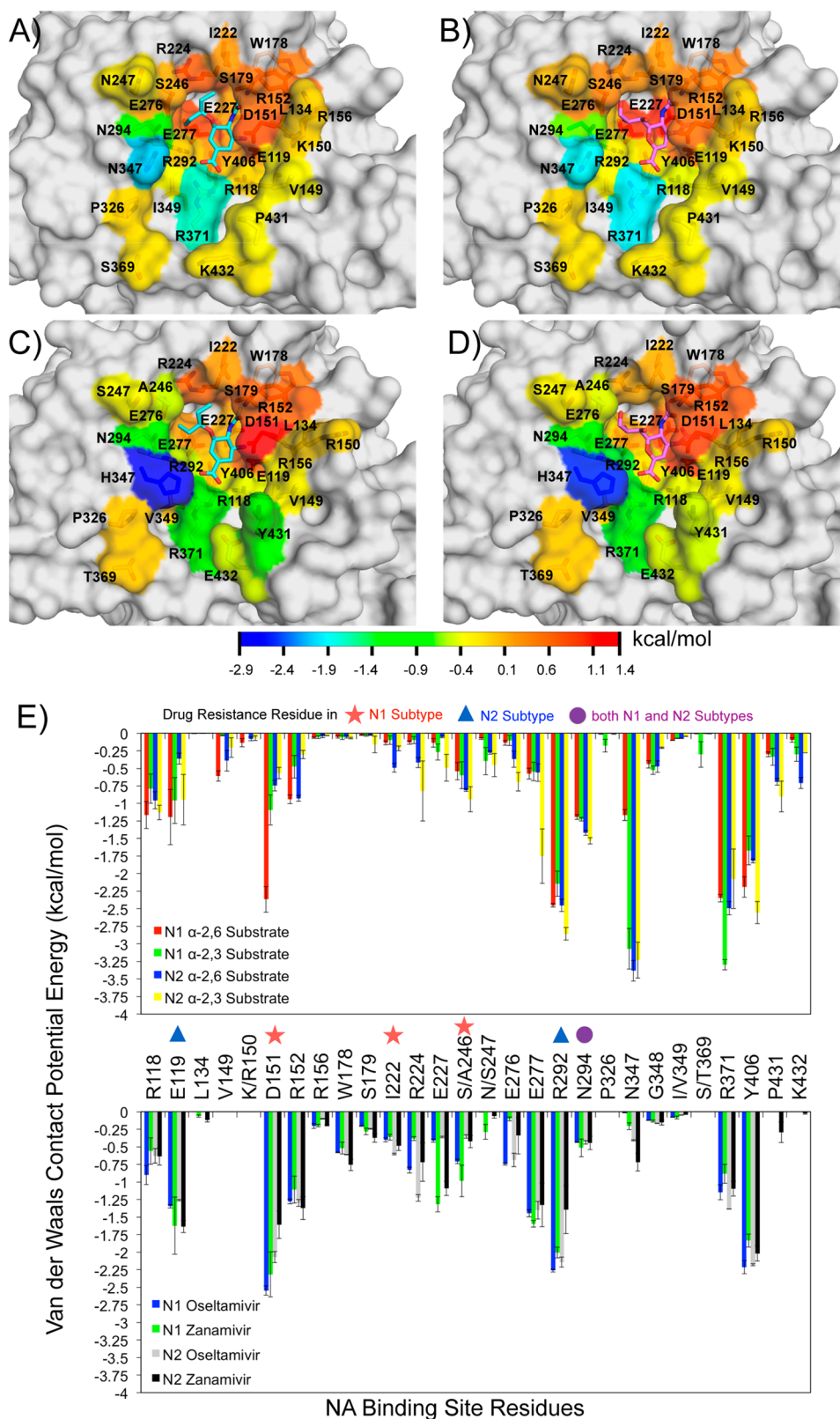


Figure 4. van der Waals interactions in NA. In panels (A–D), NA residues that contact inhibitors are colored on the surface of the active site according to differences in average vdW contact potential energies during MD simulations between substrates and the inhibitor: (A) N1 NA bound to oseltamivir, B) N1 NA bound to zanamivir, C) N2 NA bound to oseltamivir, and D) N2 NA bound to zanamivir. Oseltamivir and zanamivir are depicted as cyan and violet sticks, respectively, and NA is in gray surface representation. (E) Average vdW contact potential energies of NA active site residues.

S246N is a primary drug resistance mutation in N1 NA, but not N2, in both in vitro experiments and clinical samples.²¹

Residue 246 interacts more extensively with substrates than inhibitors in N2, and therefore this location is not an optimal

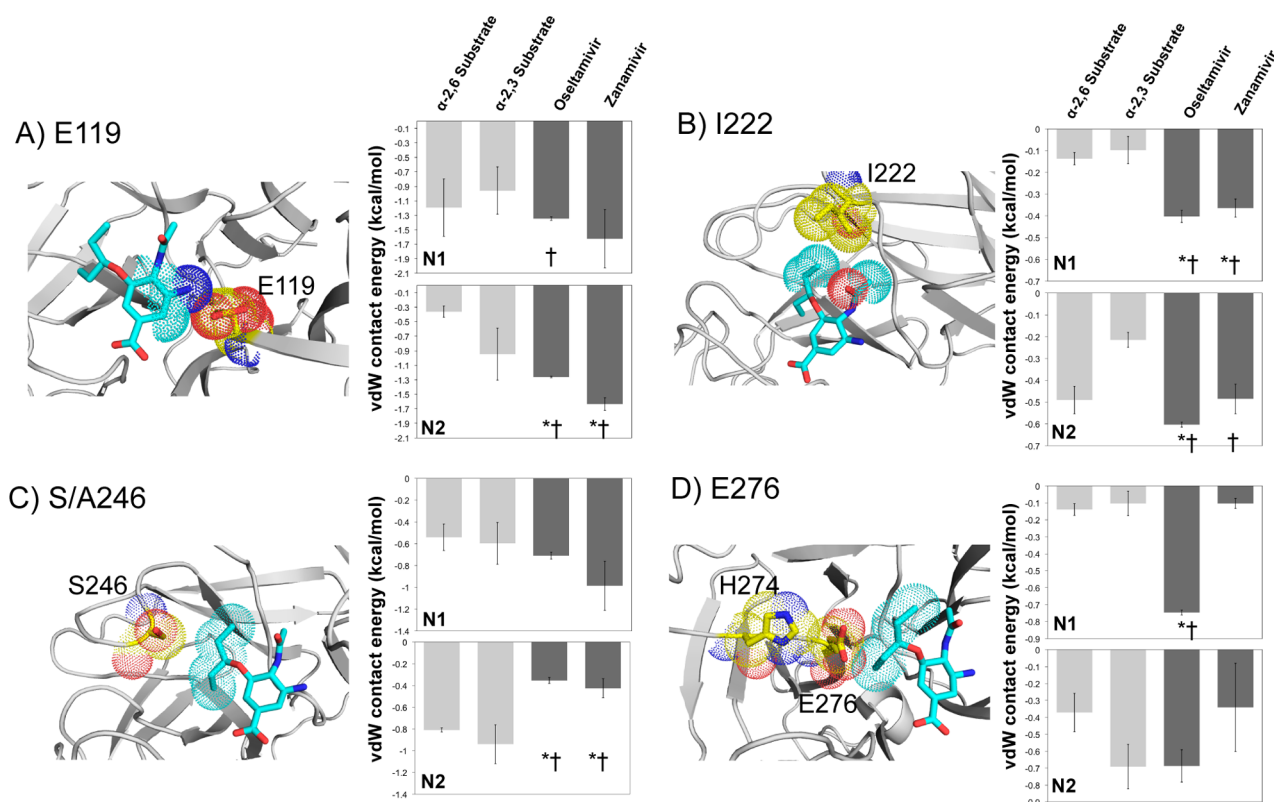


Figure 5. Differences in vdW contacts of substrates versus inhibitors underlie drug resistance sites in the two subtypes of NA. The average intermolecular vdW contact potential with (A) E119, (B) I222, (C) S/A246 (S in N1 and A in N2), and (D) E276 of the two inhibitors is compared with substrates in the bar plots, where statistically significant differences ($p < 0.05$) with α -2,3 and α -2,6 substrates are indicated by an asterisk (*) and a cross (†), respectively. In each panel, on the structure of N1 NA, the indicated residue is depicted as yellow sticks, and oseltamivir is depicted as cyan sticks, with dots showing the vdW radii of atoms.

site for resistance mutations in this subtype (Figure 5C). However, in N1, residue 246 is more important for inhibitor binding compared to substrate recognition, especially for the α -2,6 substrate. Thus, the alterations in vdW contacts in comparison to substrates correlate well with S246N being a resistance mutation in N1 only.

Susceptibility to H274Y Correlates with Intermolecular Contacts of E276. H274Y is a major oseltamivir resistance mutation in N1 NA (Table 1). Residue H274 is not directly at the active site and thus does not have any ligand contacts. The molecular mechanism underlying H274 resistance has previously been revealed by crystal structures of N1 NA: the substitution of the bulkier tyrosine pushes the E276 side chain farther into the active, which in turn pushes the bulky pentyloxy substituent of oseltamivir.⁴¹ As H274Y mutation impacts E276 at the active site, the contacts of E276 in N1 and N2 subtypes were compared to observe whether the alterations correlate with susceptibility to H274Y mutation.

Residue E276 has significantly stronger average vdW contacts with oseltamivir during the MD simulations of N1 NA compared to both substrates and zanamivir (Figure 5D). Accordingly, H274Y pushing the side chain of E276 farther into the active site would differentially impact oseltamivir binding and confer resistance, consistent with the resistance mechanism previously reported.⁴¹ In contrast, the vdW contacts of the substrates and inhibitors are not statistically different in the N2 subtype (Figure 5D). Thus, alterations in the intermolecular contacts of E276 at the active site correlate with susceptibility to H274Y mutation.

Hydrogen Bond Interactions of Substrates versus Inhibitors. In addition to the vdW contacts that report on the packing of the ligands at the active site, to better capture the intermolecular polar interactions, the hydrogen bonds between the ligands and protease active site and their stability were compared during MD simulations.

Overall, the NA substrates have fewer intermolecular hydrogen bonds than the inhibitors in both subtypes (Figure 6).⁴² The most prevalent hydrogen bonds of substrates are with residues R371, R292, and R118 and the carboxylic acid adjacent to the scissile bond in the substrates, which may help stabilize the substrate in the active site during the cleavage reaction (Figure 6B).⁴³ These three arginine residues are evolutionarily conserved in both N1 and N2 sequences (R118, R292, and R371 are 99% conserved, see Methods) and hence appear to be essential for NA function. In contrast, residues that form other hydrogen bonds with inhibitors may mutate to confer resistance.

One such residue is E119, which hydrogen bonds to inhibitors in both N1 and N2 (Figure 6). However, E119 mutations have been observed clinically only in the N2 subtype (Table 1). As explained above in vdW analysis results, this residue has comparable vdW contacts with substrates as inhibitors in N1 (Figure 5) and cannot mutate to confer resistance without compromising enzyme fitness. Hence, rather than the polar contacts, the comparative intermolecular vdW contact analysis better explains the differential resistance between the two subtypes.

A)

N1	Residue	α -2,6 Substrate	α -2,3 Substrate	Oseltamivir	Zanamivir
406	TYR	17%	25%	0%	0%
371	ARG NH2	99%	97%	78%	65%
371	ARG NH1	98%	86%	76%	38%
347	ASN	16%	39%	0%	0%
292	ARG	87%	76%	93%	71%
277	GLU	6%	4%	0%	49%
227	GLU	0%	0%	0%	98%
152	ARG	14%	11%	57%	34%
151	ASP*	18%	5%	93%	40%
119	GLU	38%	25%	81%	85%
118	ARG	73%	46%	65%	36%

N2	Residue	α -2,6 Substrate	α -2,3 Substrate	Oseltamivir	Zanamivir
406	TYR	3%	23%	0%	3%
371	ARG NH2	99%	97%	99%	65%
371	ARG NH1	98%	95%	96%	67%
347	HIS	36%	3%	0%	10%
292	ARG*	88%	100%	84%	16%
277	GLU	7%	23%	0%	24%
227	GLU	0%	0%	0%	61%
152	ARG	12%	7%	51%	48%
151	ASP	7%	10%	85%	24%
119	GLU*	10%	15%	94%	81%
118	ARG	56%	58%	36%	43%

% Occupancy

90-100%	60-69%
80-89%	50-59%
70-79%	40-49%
	<40%

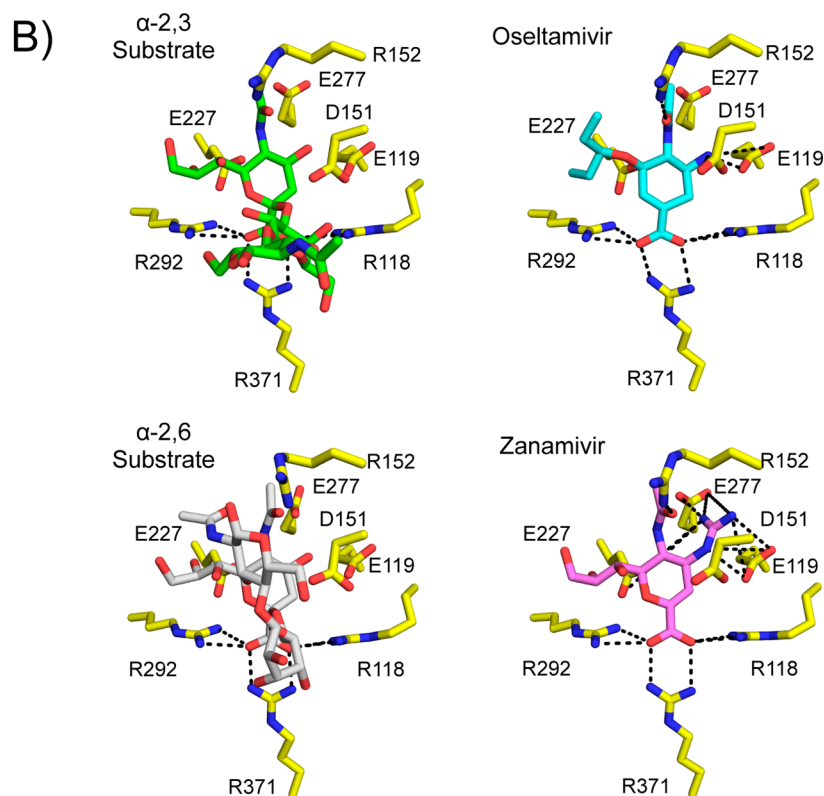


Figure 6. Intermolecular hydrogen bonding interactions during MD simulations. (A) The percentage of time that intermolecular hydrogen bonds were present during MD simulations in N1 and N2 NA, colored according to percentages. Drug resistance sites are in italics with an asterisk, and catalytic residues are in bold. (B) The residues involved in each intermolecular hydrogen bond to the four ligands are depicted as yellow sticks, and hydrogen bonds are shown with black dotted lines. The α -2,3 substrate, α -2,6 substrate, oseltamivir, and zanamivir are depicted as green, gray, cyan (blue), and violet sticks, respectively.

Another residue with stronger hydrogen bonds to the inhibitors rather than the substrates is the catalytic D151 (Figure 6). Despite being a catalytic residue, D151 can mutate to glutamic acid and conserve the charged catalytic side chain,

allowing substrate processing, but with a decreased susceptibility to oseltamivir and zanamivir in N1 NA (Table 1). D151 weakly hydrogen bonds to substrates (less than 20% and 10% of the simulation time in N1 and N2, respectively) while much

more strongly to inhibitors, especially in N1 (oseltamivir 93% and 85%; zanamivir 40% and 24% of the simulation time for N1 and N2, respectively) (Figure 6A). This differential dependence of inhibitors to hydrogen bonding in N1 NA correlates with susceptibility to D151E mutation.

In addition to pushing E276 into the active site as discussed above, the H274Y mutation causes a loss of a hydrogen bond between R152 and oseltamivir, which was proposed to be a complementary molecular mechanism in conferring resistance.⁴⁴ Mutations at R152 have also been associated with decreased NA inhibitor susceptibility.¹⁴ R152 hydrogen bonds to oseltamivir about half of the simulation time in both N1 and N2 and slightly less to zanamivir (Figure 6A). Even if the loss of this hydrogen bond is a complementary mechanism to decrease the susceptibility to H274Y once this mutation is selected,⁴⁴ there are no considerable differences in hydrogen bonding to oseltamivir versus zanamivir, or N1 versus N2, to explain the selection of H274Y in N1 only for oseltamivir.

Lastly, E227 and E277 have additional hydrogen bonds to inhibitors compared to substrates in both N1 and N2 (Figure 6A). E227 and E277 have been associated with decreased NA inhibitor susceptibility but not reported as major drug resistance sites.¹⁶ Thus, overall, losing or weakening hydrogen bonds to inhibitors compared to substrates may be a secondary mechanism underlying drug resistance, but vdW contacts beyond those of substrates more effectively explain the selection of differential pattern of drug resistance mutations in the two subtypes.

DISCUSSION

In this study, we used the *dynamic substrate envelope* and the related intermolecular interactions of substrates versus the inhibitors with the NA active site residues to explain differential patterns of drug resistance between N1 and N2 subtypes of influenza. The alterations in the vdW contact energies with NA residues between substrates versus inhibitors effectively explain the molecular basis of major resistance mutations selected in each subtype. Even though the residues in the NA active site catalytic pocket are similar between the two subtypes, the dynamically averaged interactions, specifically vdW contacts and hydrogen bonds with the substrates versus inhibitors, substantially differ at specific residues that mutate to confer differential resistance.

Drug resistance occurs when mutations selectively weaken inhibitor binding compared to substrate binding, shifting the balance away from inhibition and in favor of substrate processing. This molecular mechanism was identified to be underlying major primary drug resistance mutations in viral targets previously, in HIV-1 and HCV protease.^{33,35,45} Here, we demonstrate that the same principles apply to explaining the differential patterns of resistance mutations selected in N1 versus N2 subtype of influenza NA. We found the vdW contact energies of substrates versus inhibitors to effectively explain, while differences in hydrogen bonding can also contribute to, the selection of mutations that confer resistance in each subtype.

In addition to the mechanism discussed above for mutations at sites directly contacting inhibitors, residues away from the active site also mutate to confer resistance (Table 1, mutations not in bold). Recently, the *network hypothesis* was proposed to explain how the effect of such mutations might propagate to the active site in HIV-1 protease.⁴⁶ This hypothesis remains to be explored to reveal whether a similar mechanism can explain the

selection of NA drug resistance mutations away from the active site.

Our results suggest strategies to minimize susceptibility to resistance in the design of novel NA inhibitors. The first strategy is to avoid inhibitor contacts beyond the substrate envelope of NA. The inhibitors can be modified to avoid excess interactions with mutation-prone residues and instead gain additional interactions with residues that contact substrates more than inhibitors (Figure 4A, green-blue colors). In addition to targeting evolutionarily conserved residues essential for substrate binding, the inhibitors can fill the substrate envelope more optimally to take advantage of the remaining volume in the substrate envelope unfilled by current inhibitors (Figure 3).³⁹ In fact, the actual substrate envelope is even larger, as only the first two sugar moieties, which were ordered in the crystal structure, were included here. Although the additional extended substrate would be located outside the active site and is not likely to make any contacts with NA, this additional space could be used to modify the inhibitors to include better pharmacokinetic properties. Lastly, inhibitor rigidity may promote susceptibility to drug resistance mutations in the active site (Figure 3). Substrates can more easily accommodate binding to an active site altered due to mutations as they are more flexible, and inhibitors can be designed to better mimic these adaptable substrate dynamics. However, the high rigidity in inhibitors may also be important for tight binding interactions in the active site. Thus, inhibitors must be optimized to balance tight binding interactions that contribute to high potency while sharing critical features of substrates shared between different subtypes. In conclusion, the detailed comparative analysis of substrate and inhibitor dynamic interactions in N1 and N2 NA presented here reveals the molecular basis of differential resistance in these two influenza subtypes and presents opportunities for designing inhibitors with a higher barrier to the development of drug resistance.

MATERIALS AND METHODS

Influenza Neuraminidase Substrate and Inhibitor Complex Structures. The prototypic N1 and N2 sequences were chosen based on three criteria: 1) availability of high-quality high-resolution crystal structures, 2) high percent identity to N1 and N2 consensus sequences based on multiple sequence alignment, and 3) the presence of a “typical” 150-loop in the active site for N1 and N2.^{47,48} All of the crystal structures used in this study are of the globular head domain. Alignments were performed using the multiple sequence alignment tools on the Influenza Research Database (www.fludb.org). The strain of N2 NA used is A/Tanzania/205/2010 H3N2 NA. This strain has 94% sequence identity and 96% sequence similarity to a consensus sequence determined from an alignment of 8,745 complete and unique sequences. The strain of N1 NA used is A/Brevig Mission/1/1918 H1N1 NA. This strain has 92% sequence identity and 96% sequence similarity to a consensus sequence determined from an alignment of 7,370 complete and unique N1 NA sequences.

For N2 NA, crystal structures were available in complex with α -2,6 and α -2,3 substrates (PDB ID: 4GZX and 4GZW, respectively).¹² A crystal structure of the same strain of N2 NA was also available in complex with oseltamivir (PDB ID: 4GZP). For N1 NA, the highest quality crystal structure available of N1 NA is in complex with zanamivir (PDB ID: 3B7E).⁴⁹ Additional models were created using these four structures for cocomplex crystal structures that were unavailable

(Table S1). As is the convention in PDB files, N2 numbering was used for all structures.

Structure Preparation. Crystallographic water molecules and calcium ions were retained, and all buffer salts were removed. The substrate cocrystal structures have a D151G substitution in the active site to prevent catalysis. To more accurately model the interactions of ligands with this residue, the back-mutation G151D was modeled *in silico* using the software Maestro and Prime from Schrodinger.^{50,51} The missing D151 side chain in two of the starting N2 crystal structures (4GZW and 4GZX) was built based on the conformation in the other N2 crystal structure (4GZP) with intact D151. This side chain conformer was the same also in N1 crystal structures. After the side chain was built in, Prime (from Schrodinger Maestro Suite) was used to minimize the modeled side chain, and no changes were observed. Crystal structures were prepared using the Protein Preparation Wizard from Schrodinger.⁵²

Molecular Dynamics Simulation Protocol. For each tetrameric complex, MD simulations were collected for 100 ns using Desmond and the OPLS2005 force field.^{53,54} Each system was solvated with a 10 Å shell of TIP3P water in a truncated octahedron simulation box with periodic boundary conditions. Sodium (Na⁺) or chloride (Cl⁻) counterions were added to neutralize the overall charge of the system. Each system was first minimized to relieve steric clashes where the solute heavy atoms were restrained using a 1000 kcal mol⁻¹ Å⁻² force constant, and a hybrid method of steepest descent for up to 10 steps and of the limited-memory Broyden-Fletcher-Goldfarb-Shanno (LBFSGS) algorithm for up to 2000 steps, with a convergence threshold of 50 kcal mol⁻¹ Å⁻². Next, the system was minimized in 7 stages with a harmonic restraint on all backbone atoms that was gradually reduced from 1000 to 1 kcal mol⁻¹ Å⁻² with 5000 steps for each stage using the hybrid steepest descent LBFSGS method (250 steps steepest descent and 4750 steps LBFSGS). Lastly, a minimization without any restraints was performed, for a total of over ~40,000 minimization steps. After minimization, each system was equilibrated using a sequence of four short MD stages, following a process similar to the default relaxation for an NPT ensemble in the Desmond User Manual.⁵⁵ For the production stage, MD simulations were performed for 100 ns at 1 atm and 300 K in the NPT ensemble using a Nose-Hoover thermostat and a Martyna-Tuckerman-Klein (MTK) barostat. Long-range electrostatics were calculated using the smooth particle mesh Ewald method⁵⁶ with a cutoff radius of 9 Å. The M-SHAKE algorithm was used to implement constraints that eliminate the highest frequency vibrational motions so that longer timesteps can be used (2 fs instead of 1 fs). MD steps were integrated using a 2 fs timesteps for bonded and nonbonded interactions and 6 fs timesteps for electrostatic interactions beyond 9 Å. For each system, the trajectories of each monomer were concatenated to provide 400 ns of sampling with snapshot intervals of 200 ps for analysis.

Root Mean Squared Deviation (RMSD). Root mean squared deviation (RMSD) calculations were performed using the Visual Molecular Dynamics software package (VMD).⁵⁷ The frames from each interval were aligned to the first frame of the trajectory, and RMSD values were calculated using all backbone α carbon atoms. In addition, five N-terminal and C-terminal residues were omitted from the additional RMSD calculations to show that the approximately 375 central amino

acids of each monomer were highly stable and equilibrated rapidly.

Root Mean Squared Fluctuation (RMSF) and Simulation-Derived Temperature Factors. Root mean squared fluctuations (RMSF) and simulation-derived temperature factors (B factors) were calculated for all alpha carbons in the trajectory and averaged over 400 ns using VMD. RMSF was calculated using the built-in rmsf command in VMD, and simulation-derived B factors were calculated using the “bfactor.tcl” Tcl/Tk script. For crystal structures with more than one molecule in the asymmetric unit, temperature factors were averaged over all molecules for comparison.

Dynamic Substrate and Inhibitor Envelopes. The van der Waals (vdW) volumes of ligand conformers in the active site of each monomer from each trajectory were mapped onto a three-dimensional grid, and a probability distribution was calculated for each grid point and plotted, as described previously.³⁷

Calculation of van der Waals Contact Potential. The van der Waals contact potential energies between ligands and NA were calculated over an MD trajectory and averaged using a simplified Lennard-Jones potential function as described previously.³⁷ The nonbonded parameters were determined using the OPLS2005 force field, and values were averaged over 400 ns.

Hydrogen Bond Calculations. The percentage of time that a hydrogen bond existed during a trajectory was calculated using the HBonds Plugin from VMD and averaged over 400 ns. A hydrogen bond was defined as having a donor–acceptor distance of a maximum of 3.5 Å and involving only polar atoms nitrogen, oxygen, sulfur, and fluorine. The donor-hydrogen-acceptor angle was defined as being less than 30 degrees. Hydrogen bonds were summed over each residue and ligand except when otherwise indicated.

■ ASSOCIATED CONTENT

📄 Supporting Information

The Supporting Information is available free of charge on the ACS Publications website at DOI: 10.1021/acs.jctc.6b00703.

Table S1 and Figures S1–S4 (PDF)

■ AUTHOR INFORMATION

Corresponding Author

*E-mail: Celia.Schiffer@umassmed.edu.

Present Addresses

[∇]Genentech, San Francisco, CA.

[○]Wesleyan University, Middletown, CT.

Author Contributions

The manuscript was written through contributions of all authors. All authors have given approval to the final version of the manuscript.

Funding

This work was supported by the Office of the Assistant Secretary of Defense for Health Affairs, through the Peer Reviewed Medical Research Program (Award No. W81XWH-15-1-0317) and by the Defense Advanced Research Projects Agency (DARPA) Prophecy Program, Defense Sciences Office (DSO), Contract No. HR001111-C-0095 and D13AP00041. Opinions, interpretations, conclusions, and recommendations are those of the authors and are not necessarily endorsed by the Department of Defense.

Notes

The authors declare no competing financial interest.

ACKNOWLEDGMENTS

The authors thank Dr. Troy Whitfield for useful comments and suggestions.

ABBREVIATIONS

NA, neuraminidase; MD, molecular dynamics; vdW, van der Waals; RMSD, root mean squared deviation; RMSF, root mean squared fluctuation

REFERENCES

- (1) Molinari, N. A.; Ortega-Sanchez, I. R.; Messonnier, M. L.; Thompson, W. W.; Wortley, P. M.; Weintraub, E.; Bridges, C. B. The Annual Impact of Seasonal Influenza in the US: Measuring Disease Burden and Costs. *Vaccine* **2007**, *25*, 5086.
- (2) Carrat, F.; Flahault, A. Influenza Vaccine: The Challenge of Antigenic Drift. *Vaccine* **2007**, *25*, 6852.
- (3) Boivin, S.; Cusack, S.; Ruigrok, R. W.; Hart, D. J. Influenza A Virus Polymerase: Structural Insights into Replication and Host Adaptation Mechanisms. *J. Biol. Chem.* **2010**, *285*, 28411.
- (4) Moscona, A. Neuraminidase Inhibitors for Influenza. *N. Engl. J. Med.* **2005**, *353*, 1363.
- (5) Noll, H.; Aoyagi, T.; Orlando, J. The Structural Relationship of Sialidase to the Influenza Virus Surface. *Virology* **1962**, *18*, 154.
- (6) Palese, P.; Tobita, K.; Ueda, M.; Compans, R. W. Characterization of Temperature Sensitive Influenza Virus Mutants Defective in Neuraminidase. *Virology* **1974**, *61*, 397.
- (7) Air, G. M. Influenza Neuraminidase. *Influenza Other Respir. Viruses* **2012**, *6*, 245.
- (8) Yang, X.; Steukers, L.; Forier, K.; Xiong, R.; Braeckmans, K.; Van Reeth, K.; Nauwynck, H. A Beneficiary Role for Neuraminidase in Influenza Virus Penetration through the Respiratory Mucus. *PLoS One* **2014**, *9*, e110026.
- (9) Lew, W.; Chen, X.; Kim, C. U. Discovery and Development of Gs 4104 (Oseltamivir): An Orally Active Influenza Neuraminidase Inhibitor. *Curr. Med. Chem.* **2000**, *7*, 663.
- (10) Smee, D. F.; Sidwell, R. W. Peramivir (Bcx-1812, Rwj-270201): Potential New Therapy for Influenza. *Expert Opin. Invest. Drugs* **2002**, *11*, 859.
- (11) Woods, J. M.; Bethell, R. C.; Coates, J. A.; Healy, N.; Hiscox, S. A.; Pearson, B. A.; Ryan, D. M.; Ticehurst, J.; Tilling, J.; Walcott, S. M.; et al. 4-Guanidino-2,4-Dideoxy-2,3-Dehydro-N-Acetylneuraminic Acid Is a Highly Effective Inhibitor Both of the Sialidase (Neuraminidase) and of Growth of a Wide Range of Influenza A and B Viruses in Vitro. *Antimicrob. Agents Chemother.* **1993**, *37*, 1473.
- (12) Zhu, X.; McBride, R.; Nycholat, C. M.; Yu, W.; Paulson, J. C.; Wilson, I. A. Influenza Virus Neuraminidases with Reduced Enzymatic Activity That Avidly Bind Sialic Acid Receptors. *J. Virol.* **2012**, *86*, 13371.
- (13) Li, Y.; Cao, H.; Dao, N.; Luo, Z.; Yu, H.; Chen, Y.; Xing, Z.; Baumgarth, N.; Cardona, C.; Chen, X. High-Throughput Neuraminidase Substrate Specificity Study of Human and Avian Influenza A Viruses. *Virology* **2011**, *415*, 12.
- (14) McKimm-Breschkin, J. L. Influenza Neuraminidase Inhibitors: Antiviral Action and Mechanisms of Resistance. *Influenza Other Respir. Viruses* **2013**, *7* (1), 25.
- (15) Meijer, A.; Rebelo-de-Andrade, H.; Correia, V.; Besselaar, T.; Drager-Dayal, R.; Fry, A.; Gregory, V.; Gubareva, L.; Kageyama, T.; Lackenby, A.; Lo, J.; Odagiri, T.; Pereyaslov, D.; Siqueira, M. M.; Takashita, E.; Tashiro, M.; Wang, D.; Wong, S.; Zhang, W.; Daniels, R. S.; Hurt, A. C. Global Update on the Susceptibility of Human Influenza Viruses to Neuraminidase Inhibitors, 2012–2013. *Antiviral Res.* **2014**, *110*, 31.
- (16) Nguyen, H. T.; Fry, A. M.; Gubareva, L. V. Neuraminidase Inhibitor Resistance in Influenza Viruses and Laboratory Testing Methods. *Antiviral Ther.* **2012**, *17*, 159.
- (17) Takashita, E.; Meijer, A.; Lackenby, A.; Gubareva, L.; Rebelo-de-Andrade, H.; Besselaar, T.; Fry, A.; Gregory, V.; Leang, S. K.; Huang, W.; Lo, J.; Pereyaslov, D.; Siqueira, M. M.; Wang, D.; Mak, G. C.; Zhang, W.; Daniels, R. S.; Hurt, A. C.; Tashiro, M. Global Update on the Susceptibility of Human Influenza Viruses to Neuraminidase Inhibitors, 2013–2014. *Antiviral Res.* **2015**, *117*, 27.
- (18) Abed, Y.; Baz, M.; Boivin, G. Impact of Neuraminidase Mutations Conferring Influenza Resistance to Neuraminidase Inhibitors in the N1 and N2 Genetic Backgrounds. *Antivir. Ther.* **2006**, *11*, 971.
- (19) Orozovic, G.; Orozovic, K.; Lennerstrand, J.; Olsen, B. Detection of Resistance Mutations to Antivirals Oseltamivir and Zanamivir in Avian Influenza A Viruses Isolated from Wild Birds. *PLoS One* **2011**, *6*, e16028.
- (20) Samson, M.; Pizzorno, A.; Abed, Y.; Boivin, G. Influenza Virus Resistance to Neuraminidase Inhibitors. *Antiviral Res.* **2013**, *98*, 174.
- (21) Rameix-Welti, M.-A.; Munier, S.; Naffakh, N. In *Influenza Virus Sialidase - a Drug Discovery Target*; Itzstein, M., Ed.; Springer Basel: Basel, 2012; p 153.
- (22) Hurt, A. C.; Holien, J. K.; Parker, M.; Kelso, A.; Barr, I. G. Zanamivir-Resistant Influenza Viruses with a Novel Neuraminidase Mutation. *J. Virol.* **2009**, *83*, 10366.
- (23) Eshaghi, A.; Shalhoub, S.; Rosenfeld, P.; Li, A.; Higgins, R. R.; Stogios, P. J.; Savchenko, A.; Bastien, N.; Li, Y.; Rotstein, C.; Gubbay, J. B. Multiple Influenza A (H3N2) Mutations Conferring Resistance to Neuraminidase Inhibitors in a Bone Marrow Transplant Recipient. *Antimicrob. Agents Chemother.* **2014**, *58*, 7188.
- (24) McKimm-Breschkin, J. L.; Barrett, S.; Pudjijatmoko; Azhar, M.; Wong, F. Y.; Selleck, P.; Mohr, P. G.; McGrane, J.; Kim, M. I222 Neuraminidase Mutations Further Reduce Oseltamivir Susceptibility of Indonesian Clade 2.1 Highly Pathogenic Avian Influenza A(H5N1) Viruses. *PLoS One* **2013**, *8*, e66105.
- (25) Foll, M.; Poh, Y. P.; Renzette, N.; Ferrer-Admetlla, A.; Bank, C.; Shim, H.; Malaspina, A. S.; Ewing, G.; Liu, P.; Wegmann, D.; Caffrey, D. R.; Zeldovich, K. B.; Bolon, D. N.; Wang, J. P.; Kowalik, T. F.; Schiffer, C. A.; Finberg, R. W.; Jensen, J. D. Influenza Virus Drug Resistance: A Time-Sampled Population Genetics Perspective. *PLoS Genet.* **2014**, *10*, e1004185.
- (26) Renzette, N.; Caffrey, D. R.; Zeldovich, K. B.; Liu, P.; Gallagher, G. R.; Aiello, D.; Porter, A. J.; Kurt-Jones, E. A.; Bolon, D. N.; Poh, Y. P.; Jensen, J. D.; Schiffer, C. A.; Kowalik, T. F.; Finberg, R. W.; Wang, J. P. Evolution of the Influenza A Virus Genome During Development of Oseltamivir Resistance in Vitro. *J. Virol.* **2014**, *88*, 272.
- (27) Pan, P.; Li, L.; Li, Y.; Li, D.; Hou, T. Insights into Susceptibility of Antiviral Drugs against the E119g Mutant of 2009 Influenza A (H1N1) Neuraminidase by Molecular Dynamics Simulations and Free Energy Calculations. *Antiviral Res.* **2013**, *100*, 356.
- (28) Vergara-Jaque, A.; Poblete, H.; Lee, E. H.; Schulten, K.; Gonzalez-Nilo, F.; Chipot, C. Molecular Basis of Drug Resistance in A/H1N1 Virus. *J. Chem. Inf. Model.* **2012**, *52*, 2650.
- (29) Woods, C. J.; Malaisree, M.; Long, B.; McIntosh-Smith, S.; Mulholland, A. J. Analysis and Assay of Oseltamivir-Resistant Mutants of Influenza Neuraminidase Via Direct Observation of Drug Unbinding and Rebinding in Simulation. *Biochemistry* **2013**, *52*, 8150.
- (30) Baz, M.; Abed, Y.; McDonald, J.; Boivin, G. Characterization of Multidrug-Resistant Influenza A/H3N2 Viruses Shed During 1 Year by an Immunocompromised Child. *Clin. Infect. Dis.* **2006**, *43*, 1555.
- (31) Mishin, V. P.; Hayden, F. G.; Gubareva, L. V. Susceptibilities of Antiviral-Resistant Influenza Viruses to Novel Neuraminidase Inhibitors. *Antimicrob. Agents Chemother.* **2005**, *49*, 4515.
- (32) Pizzorno, A.; Bouhy, X.; Abed, Y.; Boivin, G. Generation and Characterization of Recombinant Pandemic Influenza A(H1N1) Viruses Resistant to Neuraminidase Inhibitors. *J. Infect. Dis.* **2011**, *203*, 25.

- (33) King, N. M.; Prabu-Jeyabalan, M.; Nalivaika, E. A.; Schiffer, C. A. Combating Susceptibility to Drug Resistance: Lessons from Hiv-1 Protease. *Chem. Biol.* **2004**, *11*, 1333.
- (34) Prabu-Jeyabalan, M.; Nalivaika, E.; Schiffer, C. A. Substrate Shape Determines Specificity of Recognition for Hiv-1 Protease: Analysis of Crystal Structures of Six Substrate Complexes. *Structure* **2002**, *10*, 369.
- (35) Romano, K. P.; Ali, A.; Royer, W. E.; Schiffer, C. A. Drug Resistance against Hcv Ns3/4a Inhibitors Is Defined by the Balance of Substrate Recognition Versus Inhibitor Binding. *Proc. Natl. Acad. Sci. U. S. A.* **2010**, *107*, 20986.
- (36) Wu, Y.; Qin, G.; Gao, F.; Liu, Y.; Vavricka, C. J.; Qi, J.; Jiang, H.; Yu, K.; Gao, G. F. Induced Opening of Influenza Virus Neuraminidase N2 150-Loop Suggests an Important Role in Inhibitor Binding. *Sci. Rep.* **2013**, *3*, 1551.
- (37) Ozen, A.; Haliloglu, T.; Schiffer, C. A. Dynamics of Preferential Substrate Recognition in Hiv-1 Protease: Redefining the Substrate Envelope. *J. Mol. Biol.* **2011**, *410*, 726.
- (38) Ozen, A.; Sherman, W.; Schiffer, C. A. Improving the Resistance Profile of Hepatitis C Ns3/4a Inhibitors: Dynamic Substrate Envelope Guided Design. *J. Chem. Theory Comput.* **2013**, *9*, 5693.
- (39) Kurt Yilmaz, N.; Swanstrom, R.; Schiffer, C. A. Improving Viral Protease Inhibitors to Counter Drug Resistance. *Trends Microbiol.* **2016**, *24*, 547.
- (40) Jiang, L.; Liu, P.; Bank, C.; Renzette, N.; Prachanronarong, K.; Yilmaz, L. S.; Caffrey, D. R.; Zeldovich, K. B.; Schiffer, C. A.; Kowalik, T. F.; Jensen, J. D.; Finberg, R. W.; Wang, J. P.; Bolon, D. N. A Balance between Inhibitor Binding and Substrate Processing Confers Influenza Drug Resistance. *J. Mol. Biol.* **2016**, *428*, 538.
- (41) Collins, P. J.; Haire, L. F.; Lin, Y. P.; Liu, J.; Russell, R. J.; Walker, P. A.; Skehel, J. J.; Martin, S. R.; Hay, A. J.; Gamblin, S. J. Crystal Structures of Oseltamivir-Resistant Influenza Virus Neuraminidase Mutants. *Nature* **2008**, *453*, 1258.
- (42) Varghese, J. N. Development of Neuraminidase Inhibitors as Anti-Influenza Virus Drugs. *Drug Dev. Res.* **1999**, *46*, 176.
- (43) Chan, J.; Bennet, A. J. In *Influenza Virus Sialidase - a Drug Discovery Target*; Itzstein, M., Ed.; Springer Basel: Basel, 2012; p 47.
- (44) Le, L.; Lee, E. H.; Hardy, D. J.; Truong, T. N.; Schulten, K. Molecular Dynamics Simulations Suggest That Electrostatic Funnel Directs Binding of Tamiflu to Influenza N1 Neuraminidases. *PLoS Comput. Biol.* **2010**, *6*, e1000939.
- (45) Romano, K. P.; Ali, A.; Aydin, C.; Soumana, D.; Ozen, A.; Deveau, L. M.; Silver, C.; Cao, H.; Newton, A.; Petropoulos, C. J.; Huang, W.; Schiffer, C. A. The Molecular Basis of Drug Resistance against Hepatitis C Virus Ns3/4a Protease Inhibitors. *PLoS Pathog.* **2012**, *8*, e1002832.
- (46) Ragland, D. A.; Nalivaika, E. A.; Nalam, M. N.; Prachanronarong, K. L.; Cao, H.; Bandaranayake, R. M.; Cai, Y.; Kurt-Yilmaz, N.; Schiffer, C. A. Drug Resistance Conferred by Mutations Outside the Active Site through Alterations in the Dynamic and Structural Ensemble of Hiv-1 Protease. *J. Am. Chem. Soc.* **2014**, *136*, 11956.
- (47) Wang, M.; Qi, J.; Liu, Y.; Vavricka, C. J.; Wu, Y.; Li, Q.; Gao, G. F. Influenza A Virus N5 Neuraminidase Has an Extended 150-Cavity. *J. Virol.* **2011**, *85*, 8431.
- (48) Amaro, R. E.; Swift, R. V.; Votapka, L.; Li, W. W.; Walker, R. C.; Bush, R. M. Mechanism of 150-Cavity Formation in Influenza Neuraminidase. *Nat. Commun.* **2011**, *2*, 388.
- (49) Xu, X.; Zhu, X.; Dwek, R. A.; Stevens, J.; Wilson, I. A. Structural Characterization of the 1918 Influenza Virus H1N1 Neuraminidase. *J. Virol.* **2008**, *82*, 10493.
- (50) *Maestro*; Schrodinger, LLC: New York, NY, 2015.
- (51) *Prime*; Schrodinger, LLC: New York, NY, 2015.
- (52) *Protein Preparation Wizard*; Schrodinger, LLC: New York, NY, 2015.
- (53) Bowers, K. J.; Chow, E.; Xu, H.; Dror, R. O.; Eastwood, M. P.; Gregersen, B. A.; Klepeis, J. L.; Kolossvary, I.; Moraes, M. A.; Sacerdoti, F. D.; Salmon, J. K.; Yibing, S.; Shaw, D. E. In *ACM/IEEE Conference on Supercomputing (SC06)* Tampa, Florida, United States, 2006.
- (54) Banks, J. L.; Beard, H. S.; Cao, Y.; Cho, A. E.; Damm, W.; Farid, R.; Felts, A. K.; Halgren, T. A.; Mainz, D. T.; Maple, J. R.; Murphy, R.; Philipp, D. M.; Repasky, M. P.; Zhang, L. Y.; Berne, B. J.; Friesner, R. A.; Gallicchio, E.; Levy, R. M. Integrated Modeling Program, Applied Chemical Theory (Impact). *J. Comput. Chem.* **2005**, *26*, 1752.
- (55) *Desmond User Manual*; Schrodinger, LLC: New York, NY, 2015.
- (56) Essmann, U.; Perera, L.; Berkowitz, M. L.; Darden, T.; Lee, H.; Pedersen, L. G. A Smooth Particle Mesh Ewald Method. *J. Chem. Phys.* **1995**, *103*, 8577.
- (57) Humphrey, W.; Dalke, A.; Schulten, K. Vmd: Visual Molecular Dynamics. *J. Mol. Graphics* **1996**, *14*, 33.